



Nanocarbon– $\{[\text{Na}_{10}(\text{PrW}_{10}\text{O}_{36})]_2 \cdot 130\text{H}_2\text{O}\}$ composite to detect toxic food coloring dyes at nanolevel

Taposhree Dutta¹ · Sabyasachi Sarkar²Received: 11 March 2016 / Accepted: 30 March 2016 / Published online: 11 April 2016
© The Author(s) 2016. This article is published with open access at Springerlink.com

Abstract Monitoring of adulterated and toxic food colors is important due to their potential toxicity and pathogenicity. Here, we report an Ln–POM (lanthanide polyoxometalate) cluster, $\{[\text{Na}_{10}(\text{PrW}_{10}\text{O}_{36})]_2 \cdot 130\text{H}_2\text{O}\}$, with carbon nano-onion (CNO) hybrid composite which is a highly efficient sensor for the rapid detection of toxic dyes like metanil yellow, auramine O, Orange II and in allura red (red 40) as low as 3.83; 4.73; 4.14 and 2.90 nmol ml⁻¹ concentration, respectively, by fluorescence spectroscopy.

Keywords Promethium–polyoxometalates · Carbon nano-onion · Nanohybrid composite Ln–POM/CNO · Toxic food color

Introduction

Serving of colorful food is esthetically pleasant to raise good appetite. To dress food material, extensive coloring materials are in use. There remain a limited number of materials recommended to be used as food color but unscrupulous uses of toxic coloring dyes are rampant for monetary profit at the cost of human lives. To control the unlawful use of harmful colors in food it is important to

detect these at ease. Thus, toxic and harmful synthetic dyes used in food, sweets, syrups, beverages, etc., should be detected early (Zhang et al. 2010). Metanil Yellow, Allura Red (red 40), Auramine O and Orange II are among the most hazardous synthetic food colors used in food to affect human health. The dye Metanil Yellow affects the central nervous system (CNS) to cause neurotoxicity (Nagaraja and Desiraju (1993); Allura red causes chromosomal damage and introduces hyperactivity and lymphoma cancer (Tanaka 1994).

Auramin O is a carcinogen which damages human eye and causes DNA damage (Parodi et al. 1982); Orange II is toxic azo dye, commonly used in organic light emitting but it affects blood cell levels (Ramchandani et al. 1994). Even at low concentration, these water-soluble dyes disturb the ecosystem and dramatically affect the vertebrates and human health (Park et al. 2009).

The rampant illegal use of these dyes because of relatively lower cost compared with the dyes recommended as food color caused serious health hazard to the consumers. Some effective measure is necessary to identify these toxic chemicals in minute quantity. To do so we have used a new hybrid system made up with nanocarbon onions—polyoxometalate, CNO/Pr–W Ln–POM, composite and used it in detecting trace amount of these toxic dyes used in food, beverages, syrup and medicines. The unique spectral, optical and electronic properties of carbon nano-onion (CNO) (Ghosh et al. 2011) and newly synthesized polyoxometalate (POM) have great potential in medicinal and industrial research with many applications in modern science and technology.

Water-soluble polyoxometalates (POMs) are an archetypical family of inorganic anionic metal oxide complex clusters which can be synthesized by relatively simple aqueous chemical processes (Müller et al. 1999). Such POMs continued to attract the interest of researchers

✉ Sabyasachi Sarkar
abya@iitk.ac.in; sabby@chem.iests.ac.in

¹ Nano Science and Synthetic Leaf Laboratory, Department of Chemistry, Indian Institute of Engineering Science and Technology, Shibpur, Botanic Garden, Howrah 711013, West Bengal, India

² Nano Science and Synthetic Leaf Laboratory, Center for Healthcare Science and Technology, Shibpur, Botanic Garden, Howrah 711013, West Bengal, India

to exploit their optical, electronic, spectral and magnetic properties for potential application in catalysis, sensors and in biomedical applications (Pope 1983; Jabbour et al. 2005; Ariga et al. 1999; Alizadeh and Tayebbe 2005). The ability of Kiggen-type heteropolyanions to form complex with lanthanide and actinide heteroatoms is, therefore, of particular relevance (Craciun and David 2001). More recently, the lanthenopolyoxometalates (Ln–POMs) have received current interest due to their special spectroscopic and magnetic properties, as well as their potential use as luminescent probes and magnetic resonance imaging agent (Yamase 1998; Xu et al. 2002; Yamase et al. 2006; Clemente-Juan et al. 1999).

On the other hand, the unique physical, chemical, spectral and optical properties of water-soluble carbon nano-onion (CNO) attracts to explore their use in composite materials for variety of applications in catalysis, biochemical sensors, engineering, and in bio-imaging (Sonkar et al. 2012). Thus, making hybrid of carbon nano-onion with POM nanoparticles may combine the properties of two ideal functional nanomaterials to get a wide range of applications which will play an important role in the development of nanoscience and nanotechnology (Suárez-Guevara et al. 2014).

In the present work, we create a water-soluble CNO/Ln–POM (Ln = Pr) hybrid composite as Ln–POM have been used to functionalize carbon nanosheets (Kume et al. 2014). We focused on the application of CNO–Pr–POM hybrid and its use to detect the trace amount of toxic color used in food materials is described herein.

Experiment

Preparation and characterization of the Ln–POM/CNO nanohybrid materials

Materials and physical measurements

All analytical grade chemicals were purchased commercially and used without further purification. Infrared spectra were recorded on a Bruker Vertex 70 FT-IR and Jasco FT-IR 460 spectrophotometer using KBr palates. UV–Visible electronic spectral measurements were carried out in water using Perkin Elmer Lambda 35 UV–Vis spectrometer and Jasco V 630 spectrometer. The luminescence spectra were recorded on Photon Technology International LPS—220B fluorescence spectrophotometer.

X-ray crystallography

Suitable diffraction quality single crystals were obtained using the slow diffusion from the crystallization procedure.

The crystals used in analysis were glued to glass fibers and mounted on a BRUKER SMART APEX diffractometer. The instrument was equipped with a CCD area detector, and data were collected using graphite-mono-chromated Mo–K α radiation ($\lambda = 0.71069 \text{ \AA}$) at low temperature (100 K). Cell constants were obtained from the least-squares refinement of three-dimensional centroids through the use of CCD recording of narrow ω rotation frames, completing almost all reciprocal space in the stated θ range. All data were collected with SMART 5.628 (BRUKER, 2003) and integrated with BRUKER SAINT program. The details of X-ray structure will be reported separately.

Synthesis of Ln–POM cluster $[Na_{10}(PrW_{10}O_{36})]_2 \cdot 130H_2O$ (I)

10 g $Na_2WO_4 \cdot 2H_2O$ (30.32 mmol) was dissolved in 20 ml distilled water (pH 8.0) in a 50-ml beaker. 1.2 g $PrCl_3 \cdot 6H_2O$ (3.385 mmol) was dissolved in 10 ml HCl and water (1:9) solution was added dropwise into the sodium tungstate in water. The pH of the final solution was adjusted to 5.0 by adding 1–2 ml dilute HCl. The light green solution was then heated to 80 °C, filtered in hot condition and then allowed cool at room temperature. After 24 h light green crystals were obtained. Yield: 6.16 g. IR spectra (KBr palate) = $\nu = 1638.43(m, \delta(H_2O))$; $931.37(m, \nu(W=O))$; $834(m)$ (W–O–W), $709.20(s)$, $582.38(s)$, $411.78 \text{ cm}^{-1}(m)$. X-ray data: formula, $H_{50}Na_{20}O_{202}Pr_2W_{20}$; formula weight; 5146.99; crystal system, triclinic; space group, $P1, Z = 4$; $a(\text{\AA}), 12.948(2)$; $b(\text{\AA}), 12.978(2)$; $c(\text{\AA}), 40.690(7)$, $\alpha(^{\circ}) 82.952(4)$; $\beta(^{\circ}) 83.288(3)$, $\gamma(^{\circ}) 77.395(3)$; $V(\text{\AA}^3), 6594(2)$; $D_{calc.} (\text{Mg/m}^{-3}) 5.18$.

Synthesis of carbon nano-onion (CNO)

Synthesis of carbon nano-onion was made by following the established procedures (Dubey et al. 2005; Ghosh et al. 2011).

Synthesis of $[Na_{10}(PrW_{10}O_{36})]_2 \cdot 130H_2O/CNO$ nanocomposite

10.0 mg carbon nano-onion was dissolved in 10 ml water. The pH of black color solution was adjusted to 7.5 by adding 1–2 ml 0.01 N NaOH solution. 4.0 mg $[Na_{10}(PrW_{10}O_{36})]_2 \cdot 130H_2O$ (Ln–POM) cluster was added into the black solution and pH of the resultant solution was adjusted to 5.5 by adding 1–2 drops of dilute HCl. The black color solution mixture of Ln–POM cluster with CNO was heated to 60 °C in the water bath and that was evaporated to dryness to yield a dry black mass. The yield was 8.52 mg.

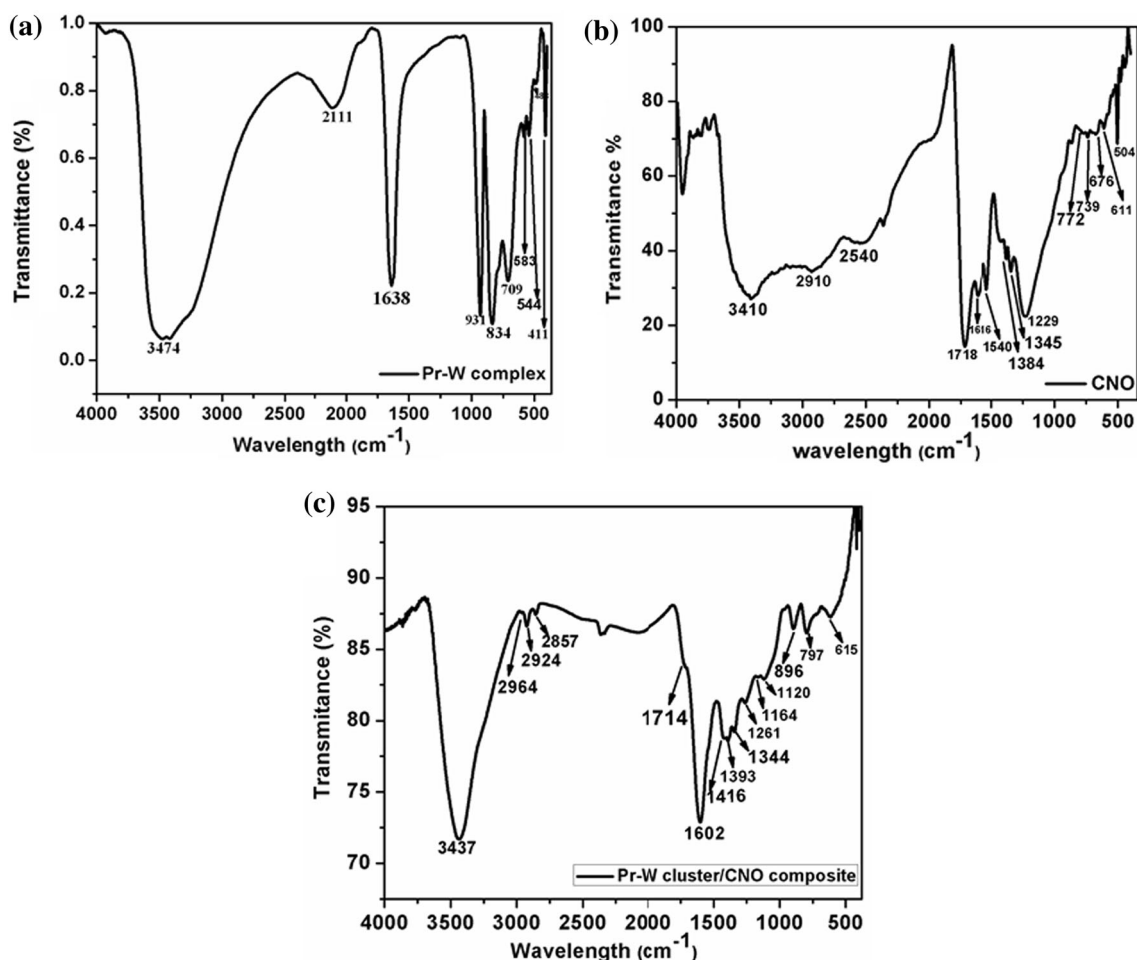


Fig. 1 IR spectra of **a** $[\text{Na}_{10}(\text{PrW}_{10}\text{O}_{36})]_2 \cdot 130\text{H}_2\text{O}$, **b** carbon nano-onion (CNO), **c** nanohybrid composite of Ln-POM cluster with CNO

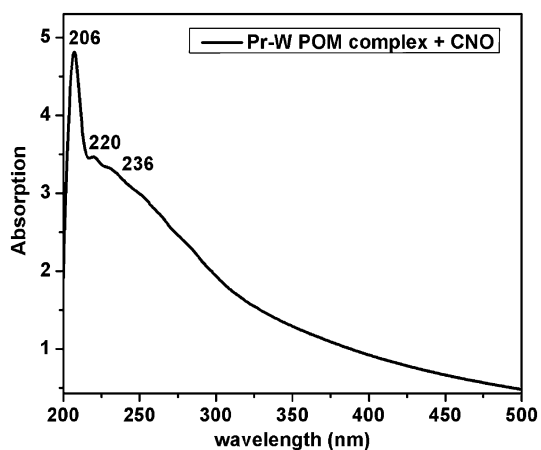


Fig. 2 Electronic spectra of nanohybrid composite of $[\text{Na}_{10}(\text{PrW}_{10}\text{O}_{36})]_2 \cdot 130\text{H}_2\text{O}/\text{CNO}$

Characterization

Complex 1 cluster is composed of $[\text{PrW}_{10}\text{O}_{36}]^{10-}$ heteropolyanions, Na^+ cations and 130 water molecules. The cluster contains an 8-coordinate promethium Pr^{III} cation sandwiched between two lacunary $[\text{W}_5\text{O}_{18}]^{5-}$ anions. The sandwich POM is connected with Na^+ cation linker. Two tungsten atoms are connected with oxygen bridge. The Pr^{III} ion is connected with 8 tungsten atoms in total (4 tungsten atom connected with oxygen atoms each side) by oxygen bridge (Ismail et al. 2009).

IR spectra

The IR spectra of Ln-POM/CNO hybrid showed the similarity to the individual spectra of POM cluster and carbon

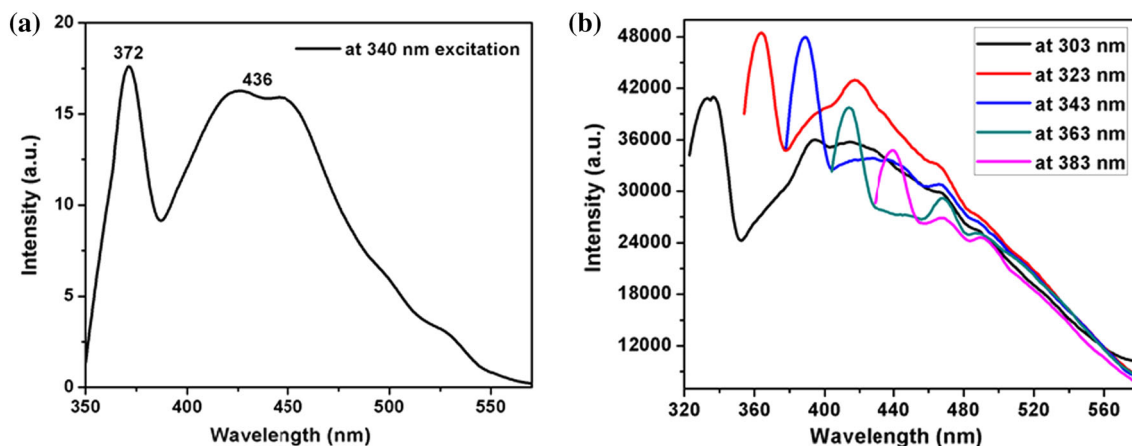


Fig. 3 Emission spectra of **a** $[\text{Na}_{10}(\text{PrW}_{10}\text{O}_{36})]_2 \cdot 130\text{H}_2\text{O}$ (Ln-POM) under excitation of 340 nm, **b** $[\text{Na}_{10}(\text{PrW}_{10}\text{O}_{36})]_2 \cdot 130\text{H}_2\text{O}/\text{CNO}$ (Ln-POM/CNO) nanohybrid composite showed several emission under varied excitation lines

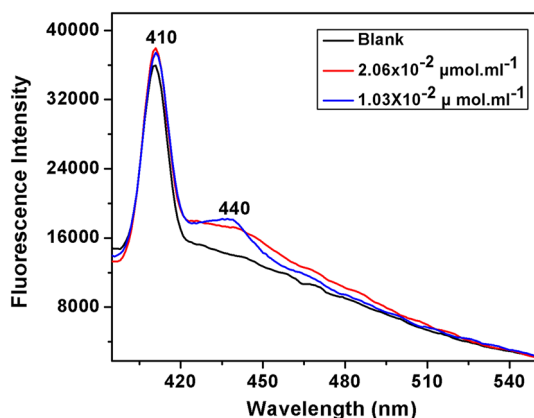


Fig. 4 Luminescence spectra of metanil yellow under varied concentration with fixed $3.43 \times 10^{-6} \text{ mol ml}^{-1}$ carbon nano-onion (CNO) showing concentration-dependent changes at 410 nm excitation where no further change occurred at lower concentration

nano-onion. The IR spectra of $[\text{Na}_{10}(\text{PrW}_{10}\text{O}_{36})]_2 \cdot 130\text{H}_2\text{O}/\text{CNO}$ nanohybrid composite and of carbon nano-onion (CNO) and lanthanide–polyoxometalate complex cluster are shown in Fig. 1. The band at 1714, 1602, 1416,

and at 1344 cm^{-1} are attributed to the C=O carboxy stretching, C=C stretching (–C–C–H) stretching and C–C stretching vibrations, respectively. Vibrations at 2964, 2924 and at 2857 cm^{-1} are attributed to the C–H vibrations and bands at 1393 and 1261 cm^{-1} are for C–C and/or (C–O) vibrations and at 1164 and at 1120 cm^{-1} are attributed to the (C–O) epoxy stretching vibrations. Bands at 896, 797 and at 615 cm^{-1} are attributed to W=O and Pr–O stretching, and W–O–W and Pr–O–W vibrations, respectively. The absorption band at 3437 cm^{-1} corresponds to the O–H stretching vibrations of water.

Luminescence property

The electronic spectrum of Ln-POM/CNO nanohybrid composite in water solvent at room temperature is shown in Fig. 2. Both $[\text{Na}_{10}(\text{PrW}_{10}\text{O}_{36})]_2 \cdot 130\text{H}_2\text{O}$ Ln-POM cluster and carbon nano-onion in isolated state display fluorescence. The Ln-POM/CNO nanohybrid composite also showed fluorescence. In Fig. 3a, the Ln-POM cluster shows two emission peaks at 372 and 436 nm, under excitation at 340 nm.

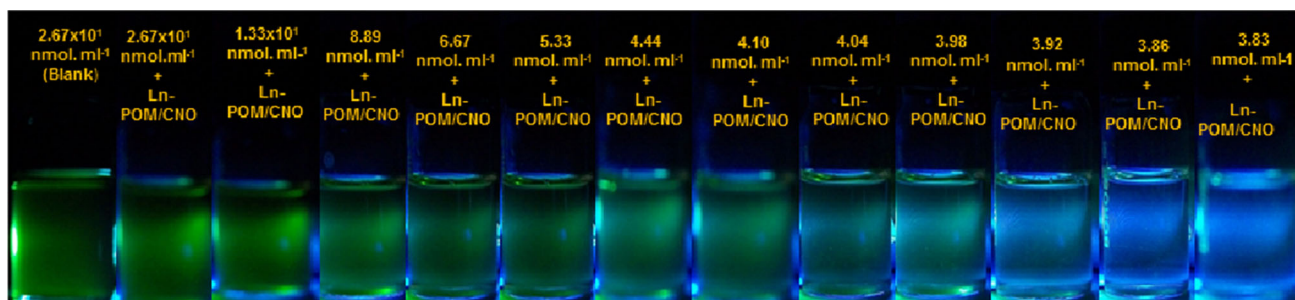


Fig. 5 Changes in fluorescence of different concentration of metanil yellow in $3.43 \times 10^{-6} \text{ mol ml}^{-1}$ aqueous solution of the Ln-POM/CNO nanocomposite

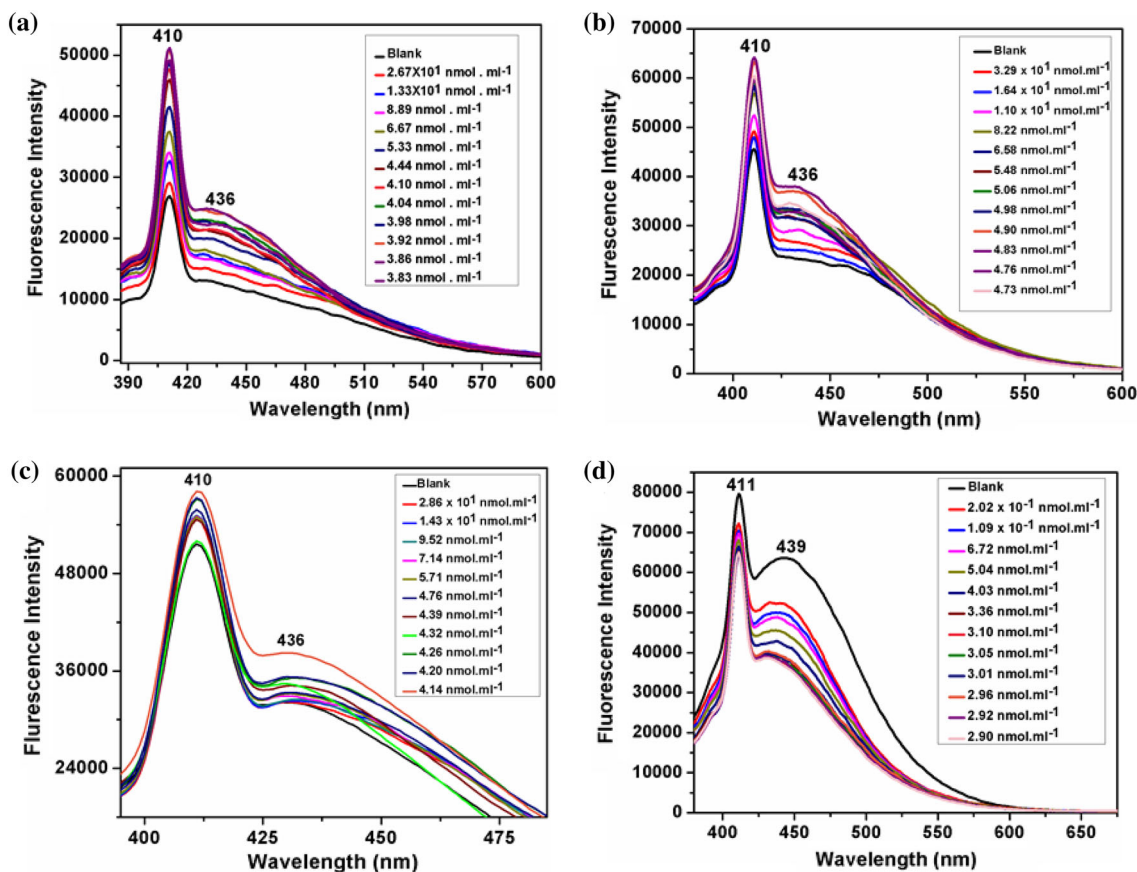


Fig. 6 Luminescence spectra of $[Na_{10}(PrW_{10}O_{36})]_2 \cdot 130H_2O/CNO$ nanocomposite with $3.43 \times 10^{-6} \text{ mol ml}^{-1}$ concentration with varied concentration of **a** metanil yellow, **b** auramine O, **c** orange II food color, **d** red 40 color dye

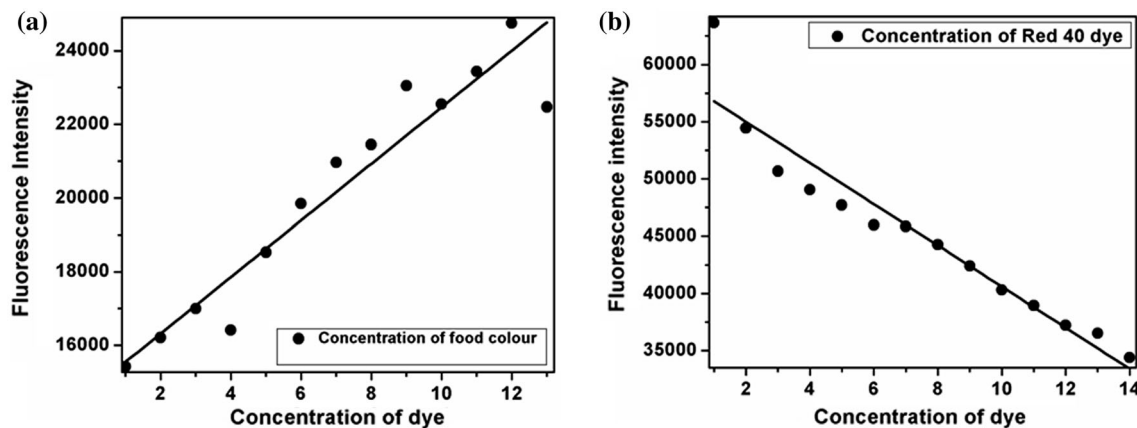


Fig. 7 Change in fluorescence intensity based on varied concentration of the food color with fixed concentration of $[Na_{10}(PrW_{10}O_{36})]_2 \cdot 130H_2O/CNO$ nanocomposite used. **a** Change in fluorescence

intensity of metanil yellow dye (similar behavior for auramine O and orange II food color, data not shown)). **b** Change in fluorescence intensity for red 40 dye

Interestingly the nanohybrid composite of Ln–POM/CNO showed fluorescence but the excitation at 323 nm excitation showed two emission peaks and the intense one is at 364 nm and a broad peak at 418 nm (Fig. 3b).

Detection of toxic colors in food through nanohybrid composite of Ln–POM cluster/CNO

Low-cost toxic colors (metanil yellow, auramine O, orange II, red 40, etc.) are banned to be used as edible stuff but are

randomly used in food stuff, i.e., sweets, biryani, veg and non-veg food stuffs with spices, ice cream, candy, medicines syrup and beverages. We tried first with metanil yellow to check the behavior of Ln–POM cluster and CNO by fluorescence spectroscopy, in the presence of 1.71×10^{-5} Ln–POM cluster with different concentration of aqueous solution of metanil yellow, no change was observed in the intensity of its yellow color; rather in the presence of 3.43×10^{-6} mol ml⁻¹ CNO, there is a change in intensity but that was in the micro range (1.03×10^{-2} μmol ml⁻¹) (Fig. 4).

We used metanil yellow to check the behavior of our composite. In the presence of 3.43×10^{-6} mol ml⁻¹ Ln–POM/CNO nanocomposite, aqueous metanil yellow showed perceptible reduction in its yellow color (not shown).

However, the variation in fluorescence can be perceptible based on the concentration of metanil yellow with a fixed concentration of the Ln–POM/CNO nanocomposite as shown in Fig. 5.

Encouraged by such an observation we performed the fluorescence study of all the four toxic dyes used under food color and data are presented in Figs. 6 and 7, respectively.

The fluorescence spectra (Fig. 6a–c) of metanil yellow, auramine O, orange II dye exhibit a strong and sharp emission peak at 410 and for red 40 at 411 nm (Fig. 6d) under excitation at 360 nm. With the fixed amount of (3.43×10^{-6} mol ml⁻¹) of [Na₁₀(PrW₁₀O₃₆)]₂·130H₂O/CNO hybrid composite and with varying concentration of toxic color chemicals the fluorescence intensity linearly changed at 410 nm in the case of metanil yellow, auramine O and orange II food colors. A concentration-dependent new emission peak albeit at lower intensity appeared at 436 nm. In the case of varied concentration of Red 40 dye, the measurable emission appeared at 411 nm and a low-intensity emission peak appeared at 439 nm instead of at 436 nm (Fig. 6). Interestingly, for the first three color dyes the fluorescence intensity steadily increased with the increase in concentration of the dye used. A representative plot of such a relationship with metanil yellow is shown in Fig. 7a. Auramine O and orange II dye showed similar behavior (data not shown). However, the behavior fluorescence intensity when red dye 40 was used shows linear dependency but reverse in order, that is, with the increase in the concentration of the dye the fluorescence intensity gets quenched steadily (Fig. 7b). Based on 3.43×10^{-6} mol ml⁻¹ of Ln–POM/CNO nanohybrid composite, we could detect toxic coloring dyes as low as 3.83 nmol ml⁻¹ for metanil yellow; 4.73 nmol ml⁻¹ for auramine O; 4.14 nmol ml⁻¹ for orange II; 2.90 nmol ml⁻¹ for red 40. Thus, the use of the hybrid composite does increase the sensitivity to detect all these food additives used as adulterated coloring materials.

Conclusion

To prevent indiscriminate use of harmful food colors, regulation has been developed by many countries; as a result, the need has arisen to continuously monitor coloring materials for permitted and non-permitted use. In the past, for both qualitative and quantitative determination techniques such as paper and thin-layer chromatography (Griffiths 1966; Goldmann et al. 2004), column chromatography (Patel et al. 1986), titration (Ashkenazi et al. 1991), electrophoresis (Yeh 1977), spectrophotometry (Prado et al. 2006; Graichen 1975) and high-performance liquid chromatography (HPLC) (Yoshioka and Ichihashi 2008) were adopted. We report here a new polyoxometalate cluster, Ln–POM, and its nanohybrid composite with carbon nano-onion. This polyoxometalate–CNO hybrid composite is used to detect four harmful and toxic colors used in coloring food items which could identify their presence in the nanolevel easily by fluorescence spectroscopy.

Acknowledgments SS thanks SERB, DST New Delhi, India for a Ramanna Fellowship (SR/S1/RFIC01/2011) to execute this project.

Open Access This article is distributed under the terms of the Creative Commons Attribution 4.0 International License (<http://creativecommons.org/licenses/by/4.0/>), which permits unrestricted use, distribution, and reproduction in any medium, provided you give appropriate credit to the original author(s) and the source, provide a link to the Creative Commons license, and indicate if changes were made.

References

- Alizadeh MH, Tayebee R (2005) Catalytic oxidation of aniline by aqueous hydrogen peroxide in the presence of some heteropolyoxometalates. *J Braz Chem Soc* 16:108–111. doi:10.1590/S0103-50532005000100017
- Ariga K, Lvov Y, Ichinose I, Kunitake T (1999) Ultrathin films of inorganic materials (SiO₂ nanoparticle, montmorillonite microplate, and molybdenum oxide) prepared by alternate layer-by-layer assembly with organic polyions. *Appl Clay Sci* 15:137–152. doi:10.1016/S0169-1317(99)00012-5
- Ashkenazi P, Yarnitzky C, Cais M (1991) Determination of synthetic food colours by means of a novel sample preparation system. *Anal Chim Acta* 248:289–299. doi:10.1016/S0003-2670(00)80898-3
- Clemente-Juan JM et al (1999) Magnetic excitations in polyoxometalate clusters observed by inelastic neutron scattering: evidence for ferromagnetic exchange interactions and spin anisotropy in the tetrameric nickel (II) cluster [Ni₄(H₂O)₂(PW₉O₃₄)₂]¹⁰⁻ and comparison with the magnetic properties. *J Am Chem Soc* 121:10021–10027. doi:10.1021/ja990197z
- Craciun C, David L (2001) Spectroscopic and magnetic investigation of one sandwich-type uranium(IV)–polyoxometalate with Ge(IV) as heteroatom. *J Alloy Compd* 323–324:743–747. doi:10.1016/S0925-8388(01)01073-8

- Dubey P, Muthukumar D, Dash S, Mukhopadhyay R, Sarkar S (2005) Synthesis and characterization of water-soluble carbon nanotubes from mustard soot. *J Phys* 65:681–697
- Ghosh M, Sonkar SK, Saxena M, Sarkar S (2011) Carbon nano-onions for imaging the life cycle of drosophila melanogaster. *Small* 7:3170–3177. doi:10.1002/sml.201101158
- Goldmann T, Taroni F, Margot P (2004) Analysis of dyes in illicit pills (amphetamine and derivatives). *J Forensic Sci* 49:716–722
- Graichen C (1975) Quantitative determination of FD&C colors in foods. *J Assoc Off Anal Chem* 58:278–282
- Griffiths MH (1966) Systematic identification of food dyes using paper chromatographic techniques. *Int J Food Sci Technol* 1:63–72. doi:10.1111/j.1365-2621.1966.tb01030.x
- Ismail AH, Dickman MH, Kortz U (2009) 22-Isopolytungstate Fragment $[H_2W_{22}O_{74}]^{14-}$ Coordinated to Lanthanide Ions. *Inorg Chem* 48:1559–1565. doi:10.1021/ic801946m
- Jabbour D, Keita B, Nadjio L, Kortz U, Mal SS (2005) The wheel-shaped $Cu_{20}Cl(OH)_{24}(H_2O)_{12}(P_8W_{48}O_{184})^{25-}$, redox and electrocatalytic properties. *Electrochem Commun* 7:841–847. doi:10.1016/j.elecom.2005.05.003
- Kume K, Kawasaki N, Wang H, Yamada T, Yoshikawa H, Awaga K (2014) Enhanced capacitor effects in polyoxometalate/graphene nanohybrid materials: a synergetic approach to high performance energy storage. *J Mater Chem A* 2:3801–3807. doi:10.1039/C3TA14569G
- Müller A et al (1999) Archimedean synthesis and magic numbers: “sizing” giant molybdenum-oxide-based molecular spheres of the keplerate type. *Angew Chem Int Ed* 38:3238–3241. doi:10.1002/(SICI)15213773(19991102)38:21<3238:AID-ANIE3238>3.0.CO;2-6
- Nagaraja TN, Desiraju T (1993) Effects of chronic consumption of metanil yellow by developing and adult rats on brain regional levels of noradrenaline, dopamine and serotonin, on acetylcholine esterase activity and on operant conditioning. *Food Chem Toxicol* 31:41–44. doi:10.1016/0278-6915(93)90177-Z
- Park M et al (2009) Risk assessment for the combinational effects of food color additives: neural progenitor cells and hippocampal neurogenesis. *J Toxicol Environ Health Part A* 72:1412–1423. doi:10.1080/15287390903212816
- Parodi S et al (1982) DNA damage induced by auramine O in liver, kidney, and bone marrow of rats and mice, and in a human cell line (alkaline elution assay and SCE induction). *J Toxicol Environ Health* 9:941–952. doi:10.1080/15287398209530216
- Patel RB, Patel MR, Patel AA, Shah AK, Patel AG (1986) Separation and determination of food colours in pharmaceutical preparations by column chromatography. *Analyst* 111:577–578
- Pope MT (1983) Heteropoly and isopoly oxometalates, vol 8. Springer Verlag
- Prado MA, Boas LFV, Bronze MR, Godoy HT (2006) Validation of methodology for simultaneous determination of synthetic dyes in alcoholic beverages by capillary electrophoresis. *J Chromatogr A* 1136:231–236. doi:10.1016/j.chroma.2006.09.071
- Ramchandani S, Das M, Khanna SK (1994) Effect of metanil yellow, orange II and their blend on hepatic xenobiotic metabolizing enzymes in rats. *Food Chem Toxicol* 32:559–563. doi:10.1016/0278-6915(94)90114-7
- Sonkar SK, Ghosh M, Roy M, Begum A, Sarkar S (2012) Carbon nano-onions as nontoxic and high-fluorescence bioimaging agent in food chain; an *In Vivo* study from unicellular *E. coli* to multicellular *C. elegans*. *Mater Express* 2:105–114. doi:10.1166/mex.2012.1064
- Suárez-Guevara J, Ruiz V, Gómez-Romero P (2014) Stable graphene-polyoxometalate nanomaterials for application in hybrid supercapacitors. *Phys Chem Chem Phys* 16:20411–20414. doi:10.1039/C4CP03321C
- Tanaka T (1994) Reproductive and neurobehavioral effects of Allura Red AC administered to mice in the diet. *Toxicology* 92:169–177
- Xu L, Zhang H, Wang E, Kurth DG, Li Z (2002) Photoluminescent multilayer films based on polyoxometalates. *J Mater Chem* 12:654–657. doi:10.1039/B108283C
- Yamase T (1998) Photo- and electrochromism of polyoxometalates and related materials. *Chem Rev* 98:307–326. doi:10.1021/cr9604043
- Yamase T, Fukaya K, Nojiri H, Ohshima Y (2006) Ferromagnetic exchange interactions for Cu_6^{12+} and Mn_6^{12+} hexagons sandwiched by two $B-\alpha-[XW_9O_{33}]^{9-}$ ($X = AsIII$ and $SbIII$) Ligands in D_{3d} -symmetric polyoxotungstates. *Inorg Chem* 45:7698–7704. doi:10.1021/ic060666f
- Yeh D-B (1977) Polyacrylamide gel electrophoresis of water-soluble coal-tar dyes. *J Chromatogr A* 132:566–568. doi:10.1016/S0021-9673(00)82925-8
- Yoshioka N, Ichihashi K (2008) Determination of 40 synthetic food colors in drinks and candies by high-performance liquid chromatography using a short column with photodiode array detection. *Talanta* 74:1408–1413. doi:10.1016/j.talanta.2007.09.015
- Zhang Y, Zhang X, Lu X, Yang J, Wu K (2010) Multi-wall carbon nanotube film-based electrochemical sensor for rapid detection of Ponceau 4R and Allura Red. *Food Chem* 122:909–913. doi:10.1016/j.foodchem.2010.03.035